Second Stable regime of Internal Kink Modes Excited by Barely Passing Energetic Ions in Tokamak Plasmas

H. D. He 1), J. Q. Dong 2,1), G. Y. Fu 3), G. Y. Zheng 1), Z. M. Sheng 2), Y. X. Long 1), Z. X. He 1), H. B. Jiang 1), Y. Shen 1) and L. F. Wang 1)
1) Southwestern Institute of Physics, Chengdu, China
2) Institute for Fusion Theory and Simulation, Zhejiang University, Hangzhou, China
3) Princeton Plasma Physics Laboratory, Princeton, USA
E-mail contact of main author: hehd@swip.ac.cn

The internal kink (fishbone) modes, driven by barely passing energetic ions (EIs), are numerically studied with the spatial distribution of the EIs taking into account. It is found that the modes with frequencies comparable to the toroidal precession frequencies are excited by resonant interaction with the EIs. Positive and negative density gradient dominating cases, corresponding to off- and near-axis depositions of neutral beam injection (NBI), respectively, are analyzed in detail. The most interesting and important feature of the modes is that there exists a second stable regime in higher β_h (=pressure of EIs / toroidal magnetic pressure) range, and the modes may only be excited by the barely passing EIs in a region of $\beta_{th1} < \beta_h < \beta_{th2}$ (β_{th} is threshold or critical beta of EIs). Besides, the unstable modes require minimum density gradients and minimum radial positions of NBI deposition. The physics mechanism for the existence of the second stable regime is discussed. The results may provide a means of reducing or even preventing the loss of NBI energetic ions and increasing the heating efficiency by adjusting the pitch angle and driving the system into the second stabile regime fast enough.

1. Introducion

The effects of energetic ions (EIs) on plasma instability and confinement in toroidal devices have been a major subject of theoretical and experimental studies in recent decades. The fish-bone like internal kink modes excited by trapped EIs have been observed in perpendicular neutral beam injection (NBI)[1] as well as ion cyclotron resonance heating (ICRH) experiments.[2-3] These modes have been analytically and numerically investigated in detail and shown to be resonantly excited by precession of deeply trapped EIs.[4-7] Besides the low frequency fish-bone modes, high frequency internal kink modes, being resonantly destabilized by passing EIs, have also been observed in tangential NBI experiments.[8] These instabilities usually result in loss of the EIs, and consequently degradation of confinement and efficiency of plasma heating. Therefore, it is crucially important to control and to avoid the instabilities in advanced tokamak experiments. On the other hand, experimental and theoretical studies have shown that a population of energetic trapped ions can result in plasma completely stable to both sawtooth oscillations and the fishbone mode.[9-11] In this work, the unstable modes driven by barely passing EIs are investigated, taking the spatial density distribution of EIs into account. The frequency of the modes is found to increase dramatically when the radial profile of the EI density changes from off-axis peaking to near-axis peaking. The mode growth rate as a function of β_h, has a maximum and, therefore, there exits a second stable regime in higher β_h range.

2. Dispersion relation

A larger-aspect-ratio tokamak plasma consisting of core and hot (energetic) components is considered. The inverse aspect ratio is $\varepsilon = a/R << 1$ (here a and R are minor and major radii of the torus, respectively). The following orderings are assumed in this paper in accordance

with tokamak experiments: $\beta_{pc} \sim O(1)$, $\beta_{ph} \sim O(\varepsilon)$, ($\beta_{pc}$ is the poloidal beta value of the core component), and the temperature ratio between the core and hot components, $T_c / T_h \sim O(\varepsilon^2)$. Therefore, the density ratio between the energetic and the core components is estimated as $n_h / n_c \sim O(\varepsilon^3)$. By making use of these assumptions, a dispersion function is obtained as ,[4-5]

$$D(\omega) = \delta W_{MHD} + \delta W_k + \delta_I , \qquad (1)$$

Where $\delta_I = -\frac{1}{2}\omega^2 \int d^3x \rho_m \left|\xi\right|^2$ is the inertial term, δW_{MHD} and δW_k are MHD and kinetic contributions, respectively, given by the following two equations,

$$\delta W_{MHD} = -\frac{1}{2}\int d^3x [\frac{\left|\delta B_\perp\right|^2}{4\pi} - \frac{j_{//}}{c}(\vec{\xi}_\perp^* \times \vec{e}_{//}) \bullet \delta\vec{B}_\perp - 2(\vec{\xi}_\perp \bullet \nabla P)(\vec{\xi}_\perp^* \times \vec{\kappa}) + \frac{B^2}{4\pi}\left|\nabla \bullet \vec{\xi}_\perp + 2\vec{\xi}_\perp \bullet \vec{\kappa}\right|^2 + \gamma P_c \left|\nabla \bullet \vec{\xi}_\perp\right|^2], \quad (2)$$

$$\delta W_k = 2^{9/2}\pi^3 m_h \int RBrdr \int d\alpha \int_0^\infty dE E^{5/2} K_b \frac{\bar{J}_0^* Q \bar{J}_0}{\omega_d - \omega} . \qquad (3)$$

Here, $K_b = \frac{1}{2\pi}\oint \frac{d\theta}{\sqrt{1-\alpha B}}$, $Q = (\omega \frac{\partial}{\partial E} + \hat{\omega}_{*h})F$, $J = \frac{\alpha B}{2}\nabla \bullet \vec{\xi}_\perp - (1 - \frac{3\alpha B}{2})\vec{\xi}_\perp \bullet \vec{\kappa}$ with $\vec{\kappa} = \vec{b} \bullet \nabla \vec{b}$ being the curvature of the magnetic field line, E is energy of EIs , $\hat{\omega}_{*h} = \omega_{*h} / T_h$, T_h is temperature of EIs. $\omega_{*h} = -iT_h /(m_h \omega_0)(\vec{b} \times \nabla \ln F) \bullet \nabla$ is the diamagnetic drift frequency of EIs, $\bar{A} = (\oint A dl / \left|v_{//}\right|) / (\oint dl / \left|v_{//}\right|)$ is an average over a field line, $\alpha = \mu / E$ (μ is magnetic moment) and ω_0 are the pitch angle and cyclotron frequency of the EIs, respectively, and $F(r, \alpha, E) = n(r)\delta(\alpha - \alpha_0)g(E)$ is the distribution function of the EIs. In addition, the transit frequency ω_t is neglected in Eq. (3) due to the fact that barely passing EIs are considered only. The radial density profile is assumed to be $n(r) \sim e^{-\sigma^2 (r - r_0)^2}$ and a slowing-down energy distribution $g(E) = E^{-3/2}$ is employed for the EIs. $\omega_d = (Eq / r\omega_0 R)K_c$ is the bounce averaged precession frequency of the EIs. K_c is a function of the first and the second kinds of complete elliptic functions E and K

$$K_c = 1 + 2k^2[\frac{\mathrm{E}(1/k)}{\mathrm{K}(1/k)} - 1] + 4k^2 s[\frac{\mathrm{E}(1/k)}{\mathrm{K}(1/k)} - \frac{\pi}{2\mathrm{K}(1/k)}\sqrt{1 - 1/k^2}] \qquad (4)$$

with the argument $k^2 = (1/\alpha_0 - 1 + r/R)/(2r/R)$ for passing particles,[12-13] here, and $s = rdq/qdr$ is magnetic shear. The average beta value of the EIs inside the q=1 flux surface may be expressed as

$$\beta_h = \int d^3x 8\pi (\int d^3v EF) / B^2 V = c_\beta \int r dr d(\alpha B) E f(r, \alpha, E) K_b dE , \quad (5)$$

where V is the volume of plasma column, $f(r, \alpha, E) = 2^{5/2} R\sqrt{E} F(r, \alpha, E) / N_p$ is the normalized distribution function, N_p is the total number of the EIs, and $c_\beta = \frac{2\pi^2 N_p}{RB^2 r_s^2}$. The third term on the right hand side in Eq.(2) indicates that the contribution of the hot particles to δW_{MHD} is $\delta W_{MHD,h} = -\int d^3x (\vec{\xi}_\perp \bullet \nabla P)(\vec{\xi}_\perp^* \bullet \kappa))$. In order to minimize the dispersion function Eq.(1), an appropriate trial function is constructed as $\vec{\xi}_\perp = (\vec{e}_r + i\vec{e}_\theta)\xi_0 \exp(i\theta - i\phi)$ inside the q=1 flux surface of radius r_s and $\vec{\xi}_\perp = 0$ outside the surface. Note, the toroidal and poloidal wave vectors as well as the radial structure of the mode under consideration are all fixed with this trial function. Following the minimizing procedure described in Refs.4-5, the dispersion relation is obtained as following from Eqs.(1-3),

$$0 = D(\omega) \equiv -i\frac{\omega}{\omega_A} + \delta\hat{W}_c + \delta\hat{W}_{MHD,h} + \delta\hat{W}_k , \qquad (6)$$

where the normalization $\delta\hat{W} = 2R\delta W / (\pi B^2 r_s^2 \xi_0^2)$ has been introduced and

$\delta\hat{W}_c = 3\pi\Delta q(r_s/R)^2(13/144-\beta_{ps}^2)$ is obtained [14] with $\beta_{ps} = -(\frac{R}{r_s^2})^2\int_0^{r_s} r^2\beta' dr$, $\Delta q = 1-q(0)$, and $\beta = 8\pi P/B_0^2$ is the beta value of the core component. After integrated over energy E and pitch angle α, Eq. (6) becomes,

$$0 = D(\omega) \equiv -i\frac{\omega}{\omega_A} + \delta\hat{W}_c + \delta\hat{W}_{k0} + \delta\hat{W}_{k1}. \qquad (7)$$

Here, the responses $\delta\hat{W}_{k0}$ and $\delta\hat{W}_{k1}$ are damping and driving terms and given by the following two equations, respectively,

$$\delta\hat{W}_{k0} = \frac{\beta_h R n(r_s)}{2r_s a'}(\frac{2\mathrm{E}}{\mathrm{K}}-1) + \frac{\beta_h R}{2r_s a'}\hat{C}\int_0^1 n(\hat{r})\sqrt{\frac{1}{\hat{r}}}d\hat{r} \qquad (8)$$

$$\delta\hat{W}_{k1} = -\frac{\beta_h R}{2r_s a'}(\frac{2\mathrm{E}}{\mathrm{K}}-1)^2\frac{\Delta n}{qK_c}[1+\Omega\ln(1-\frac{1}{\Omega})] + \frac{\beta_h R}{2r_s a'}\Omega(\hat{A}-\hat{B}-\hat{B}\Omega\frac{\partial}{\partial\Omega})\int_0^1 n(\hat{r})\sqrt{\hat{r}}\ln(1-\frac{1}{\Omega\hat{r}})d\hat{r} \qquad (9)$$

with $a' = \int_0^1 n(\hat{r})\sqrt{\hat{r}}d\hat{r}$, $\Omega = \omega/\omega_{ds}$, $\Delta n = n(r_s)-n(0)$. We can evaluate the threshold beta of EIs by letting $\Omega = \Omega_r + i\gamma$, $\gamma \to 0$. Considering that $\ln(x) = \ln|x| + i\pi$ when $x<0$, an expression for the threshold beta can be easily obtained as following by letting $\mathrm{Im}\, D(\omega) = 0$,

$$\beta_{h,crit} = \frac{2r_s a'\omega_{ds}}{\pi\omega_A R(\hat{A}-\hat{B}-\hat{B}\Omega_r\frac{\partial}{\partial\Omega_r})\int_0^{1/\Omega_r} n(\hat{r})\sqrt{\hat{r}}d\hat{r}}, \qquad (10)$$

where $\Omega_r > 1$ has to be determined by substituting Eq. (10) back into the real part of Eq. (7).

The normalized $\hat{A}$, $\hat{B}$, $\hat{C}$ are given as,

$$\hat{A} = (\frac{1-2k^2}{K_c}-\frac{1}{\alpha})(\frac{2\mathrm{E}}{\mathrm{K}}-1)[\frac{d}{dk^2}(\frac{\mathrm{E}}{\mathrm{K}}) + \frac{1}{2\mathrm{K}}\frac{d(2\mathrm{E}-\mathrm{K})}{dk^2}] + \frac{(2\mathrm{E}/\mathrm{K}-1)^2}{2K_c}(1-\frac{1-2k^2}{K_c}\frac{dK_c}{dk^2}), \qquad (11)$$

$$\hat{B} = \frac{(2\mathrm{E}/\mathrm{K}-1)^2}{2K_c}[(\frac{1-2k^2}{K_c}-\frac{1}{\alpha})\frac{dK_c}{dk^2}-2], \qquad (12)$$

$$\hat{C} = (\frac{2\mathrm{E}/\mathrm{K}-1}{K_c}-1)[\frac{1}{2}(\frac{2\mathrm{E}}{\mathrm{K}}-1) + \frac{1-2k^2}{2\mathrm{K}}\frac{d(2\mathrm{E}-\mathrm{K})}{dk^2}] + \frac{(2\mathrm{E}/\mathrm{K}-1)(1-2k^2)}{2K_c}[\frac{d}{dk^2}(\frac{2\mathrm{E}}{\mathrm{K}}) - \frac{(2\mathrm{E}-\mathrm{K})}{K_c\mathrm{K}}\frac{dK_c}{dk^2}] \qquad (13)$$

3. Numerical results

We consider a neutral beam injection experiment (injection energy E_b=60KeV) on the HL-2A tokamak[15] with a circular cross section equilibrium configuration. The other parameters are the toroidal magnetic field B_t=1.68T, the major radius R=165cm, the minor radius a=40cm, the magnetic shear s=0.003, the Alfven frequency $\omega_A = 4.31\times10^6$ s^{-1}, $\hat{r}_0$=0.72/0.25 corresponding to the cases that positive/negative radial gradient of the energetic ion density dominates (i.e. off-axis/near-axis NBI heating, respectively). $\delta\hat{W}_c = 0.003$ (i.e. MHD is stable) and the q=1 surface is located at r_s=a/2. Under these conditions, the particles with $0 < \alpha_0 < 1-r_s/R$ (or k>1) are passing particles.

The dispersion relation, Eq. (7) is numerically solved and an unstable mode is found to be driven by barely passing EIs. The real frequency ω_r and growth rate γ of the mode versus β_h are given in Fig.1 where the lines with open circles denote modes in the high frequency range whereas the lines without symbols do that in the low frequency range. Meanwhile, the dashed, the dash-dotted and the solid lines correspond to σ=6, 7, 7.5, respectively, with α_0=0.8, $\hat{r}_0$=0.25 for the modes with higher frequencies, and α_0=0.8, 0.78,

0.76, respectively with σ=2.5, $\hat{r}_0$=0.72 for the modes with lower frequencies. Generally speaking, the modes are unstable in the lower and higher frequency ranges for off-axis peaking and near-axis peaking density profiles, respectively. The striking feature of the modes studied here is that there exists a second stable regime in the higher β_h parameter range and, therefore, there are two threshold beta values, β_{th1} and β_{th2}. The instability is excited by barely passing energetic ions when the condition $\beta_h > \beta_{th1}$ is satisfied. The growth rate increases first, and then decreases gradually after reaching a maximum when β_h increases. Finally, the mode becomes stable when $\beta > \beta_{th2}$. The real frequency of the mode is comparable to the toroidal precession frequency ω_d indicats that the resonant excitation is dominant. The expression of ω_d above indicates that it is inversely proportional to radial position *r*. Therefore, the modes in high and low frequency ranges are driven unstable, respectively, when the radial profile of the EI density changes from near-axis peaking to off-axis peaking. This figure also indicates that the higher the σ value, the wider the unstable range of β_h for fixed α_0=0.8, and $\hat{r}_0$=0.25. On the other hand, the lower the α_0 value, the wider the unstable range for fixed σ=2.5, $\hat{r}_0$=0.72 and the parameter α_0 domain studied here.

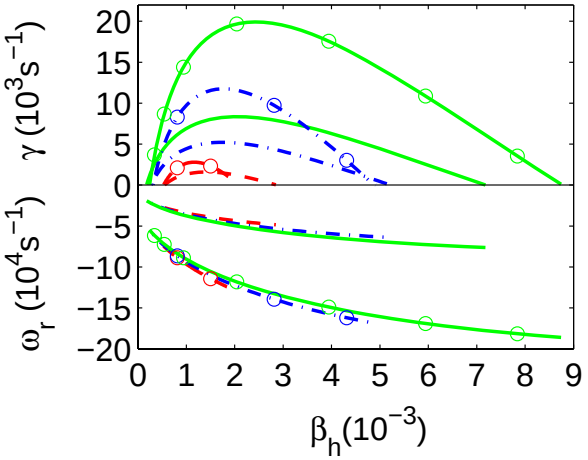

FIG. 1. The mode real frequency ω_r and growth rate γ as functions of β_h, the lines with circles and without symbols denote the modes in high frequency and low frequency ranges, respectively.

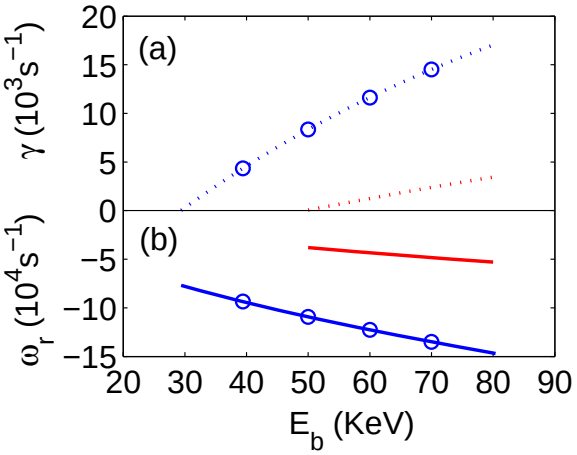

FIG. 2. The real frequency ω_r and growth rate γ as functions of the beam energy E_b for off-axis heating and near-axis heating.

Shown in Fig. 2 are the real frequency ω_r and growth rate γ as functions of beam energy E_b with $\beta_h = 0.002$ and $\alpha_0 = 0.8$. The lines with circles correspond to near-axis heating with $\hat{r}_0$=0.25, σ=7 and the other lines correspond to off-axis heating with $\hat{r}_0$=0.72, σ=2.5. It is clear that the growth rate increases monotonically with increasing beam energy when β_h is kept constant. Consequently, there exists a critical E_b for both near-axis and off-axis heating cases. In addition, the critical beam energy for near-axis heating case is about 3/5 of that for off-axis heating case.

Given in Fig.3 are the dependences of the real frequency (the solid lines) and the growth rate (the dash-dotted lines) on the deposition position $\hat{r}_0$ (the lines with triangles) of NBI for σ=7.5 and on the density gradient parameter σ (the lines with circles) for $\hat{r}_0$=0.25. The results clearly indicate that there exists a critical value, $\hat{r}_0 = \hat{r}_{0crit}$. When $\hat{r}_0 > \hat{r}_{0crit}$, the mode is excited and the growth rate increases first, reaches a maximum value, and then decreases with

further increase of $\hat{r}_0$. The real frequency monotonically decreases with increasing of $\hat{r}_0$ from high frequency range to low frequency range. The formula $-\omega_r \sim c/\hat{r}_0$ (here c is a scaling constant) fits the numerical results quite well as shown by the dotted line, showing the same scaling with $\hat{r}_0$ as the precession frequency ω_d does. The growth rate and the real frequency of the mode for $\hat{r}_0$=1.0 are both much lower than the maxima reached at $\hat{r}_0$~0.3 and 0.2, respectively. This indicates that the mode is easier to be destabilized for $\partial F/\partial r < 0$ dominating (near-axis heating) case than for $\partial F/\partial r > 0$ dominating (off-axis heating) case. For both off-axis and near-axis heating cases, the resonant energy exchanging between the hot ions and the modes plays an essential role in excitation of the mode with frequency comparable to ω_d.

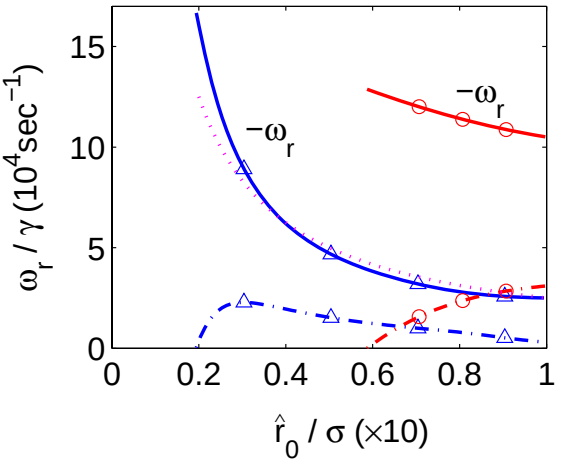

FIG. 3. The real frequency ω_r (the solid lines) and growth rate γ (the dash-dotted lines) as functions of $\hat{r}_0$ (the lines with triangles) and density gradient parameter σ (the lines with circles) with α_0=0.8, β_h=0.002. $\hat{r}_0$=0.25 for the lines with circles and σ=7.5 for the lines with triangles. The dotted line is a fit of $-\omega_r \sim c/\hat{r}_0$

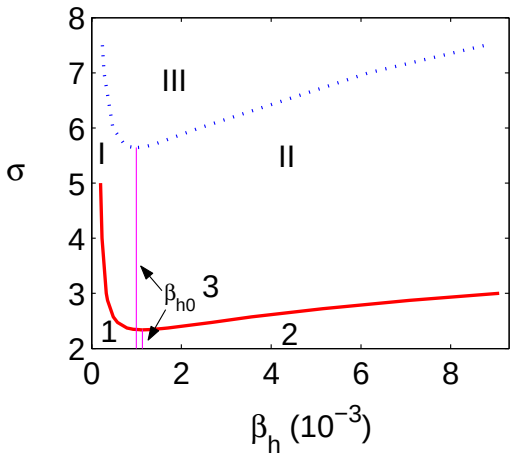

FIG.4. The stability diagrams in the $\beta_h - \sigma$ plane. The solid and dotted lines are for the modes in off-/near-axis heating cases with $\hat{r}_0$=0.72/0.25 and α_0=0.80.

In addition, the lines with circles indicate that a minimum $\sigma_{crit} \sim 6$ is also necessary to drive the mode unstable while the real frequency $\omega_r \sim 1.2\times10^5$/s does not vary much up to $\sigma \sim 10$ for $\hat{r}_0$=0.25. The minimum $\sigma_{crit} \sim 2.5$ is also required to drive the mode unstable and the real frequency $\omega_r \sim 4\times10^4$/s does not vary much up to $\sigma \sim 10$ for $\hat{r}_0$=0.72 (not shown here).

Shown in Fig.4 are the stability diagrams in the $\beta_h - \sigma$ plane. The solid and dotted lines correspond to $\hat{r}_0$=0.72 and $\hat{r}_0$=0.25, respectively, with α_0=0.80 for both cases. The $\beta_h - \sigma$ plane is divided into unstable and stable regions by each curve. The mode is unstable and stable above and below the corresponding line, respectively, in each case. Beta values on the curves are critical beta values $\beta_{h,crit}$ for each case. There are two critical beta values for a given σ in each case. The ranges in Fig.4 marked with numbers 1, 2 and 3 for off-axis heating case (I, II and III for near-axis heating case) are called the first, the second stable ranges and the unstable ranges, respectively. In each first stable range, the mode can be driven on the condition that the hot particle beta is higher than the critical value. On the contrary, the mode

becomes stable when beta is higher than the second critical value and enters into the second stability range. From Fig.4 we can see that the first threshold beta value of energetic ions decreases with increasing σ whereas the second one increases with increasing σ for both near- and off-axis heating cases. This indicates that the mode is difficult to be driven unstable but easy to enter the second stability regime for flat density profiles of EIs. It is the opposite for peaked density profiles. In addition, steeper density profiles are needed to drive the modes in high frequency range (i.e. in near-axis heating case) than that in low frequency range (i.e. off-axis heating case).

Furthermore, it is numerically found that there exist minimum values of density gradient parameter $\sigma = \sigma_{min}$ in the vicinity of $\beta_h = \beta_{h0} \sim 1.0 \times 10^{-3}$ for the both. The barely passing EIs can destabilize the modes through wave-particle resonance only when $\sigma > \sigma_{crit}$.

Nyquist technique is employed to further check the results presented above. Shown in Fig. 5 are the Nyquist diagrams plotted in the complex $D(\omega)$ plane. The dashed and the dash-dotted lines are for two β_h values in the first and second stable regions, whereas the dotted line is for one β_h in the unstable region. The diagrams clearly demonstrate that there is indeed an unstable mode (the curve encircles the original point once) only when β_h is higher than the first threshold beta value and lower than the second one. Otherwise, there are no unstable modes (the curve does not encircle the original point). Therefore, results in Fig.(1) are confirmed.

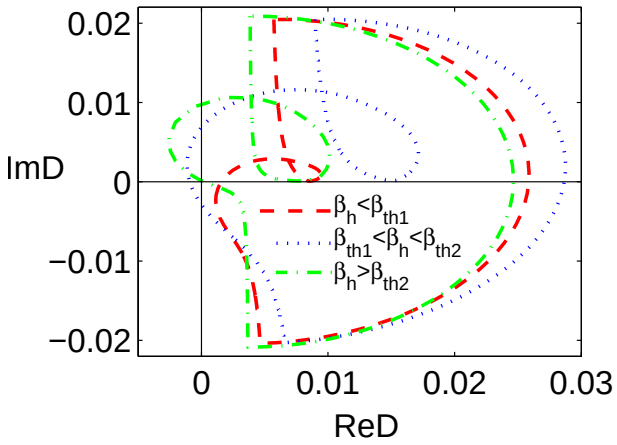

FIG.5 the Nyquist diagrams plotted in the complex D plane. The dashed, dash-dotted and dotted lines are, respectively, for the first, the second stable regions and the unstable region.

4. The possible physical mechanism

It is worthwhile to discuss the physical mechanism for the formation of the second stable regime of the modes more in detail. Taking an off-axis heating case with σ=2.5, $\hat{r}_0$=0.72 as an example, shown in Fig.6 (a) is the damping term $\delta\hat{W}_{k0}$ in Eq. (7) as a function of α_0 covering both passing and trapped ranges for β_h=0.002. The results indicate that the damping effect of $\delta\hat{W}_{k0}$ in the passing range (the solid line) is much stronger than that in the trapped range (the broken line). This may mean that the modes excited by passing EIs are easier to enter into the second stability region than that done by trapped EIs. On the other hand, roughly speaking, the real part of the driving term $\delta\hat{W}_{k1}$ in Eq.(7) provides necessary free energy for inducing the unstable modes. The exciting condition for the unstable modes to develop may be estimated as $\delta\hat{W}_c + \delta\hat{W}_{k0} + \mathrm{Re}(\delta\hat{W}_{k1}) < 0$ from Equation (7). That is, the free energy provided by the driving term is greater than the damping term $\delta\hat{W}_{k0}$ plus core MHD term $\delta\hat{W}_c$. Shown in Fig.6 (b) is the

dependence of $\delta W_k^R = \delta\hat{W}_c + \delta\hat{W}_{k0} + \mathrm{Re}(\delta\hat{W}_{k1})$ on β_h. The solid and broken lines are for barely passing ions with α_0 =0.76 and barely trapped ions with α_0 =0.93, respectively. δW_k^R decreases monotonically, meaning the mode becomes more unstable, with increasing of β_h for barely trapped EIs of α_0 =0.93. In contrast, δW_k^R decreases first, reaches a minimum and then increases with increasing of β_h for barely passing EIs of α_0 =0.76. In addition, we learn from equation (8) that the damping term depends on β_h linearly and is independent of the mode frequency and growth rate. Consequently, the contribution of damping term is trivial for small β_h and predominant for large β_h. This is the reason why the absolute value of δW_k^R in Fig.6 (b) increases with increasing β_h in the small β_h range and decreases in the large β_h range. As a result, the mode is driven unstable for small β_h. On the other hand, the destabilizing effect of energetic ions can be greatly weakened by the damping term $\delta\hat{W}_{k0}$ for large beta. Therefore，it is understandable that the growth rate in Fig.1 increases for small beta and decreases after reaching a maximum γ for large beta when β_h increases. It is also clear that there is not a second stable regime for the internal kink (fishbone) modes driven by deeply trapped EIs since the free energy δW_k^R monotonically increases with β_h for trapped EI case. The main features of the modes, such as possessing second stable regime, remain for radial density profile, $n(\hat{r}) \sim e^{-\sigma^2(\hat{r}^2-\hat{r}_0^2)^2}$, which provide zero density gradient at the original point of $\hat{r}_0 = 0$ and prevents non-physical factors.

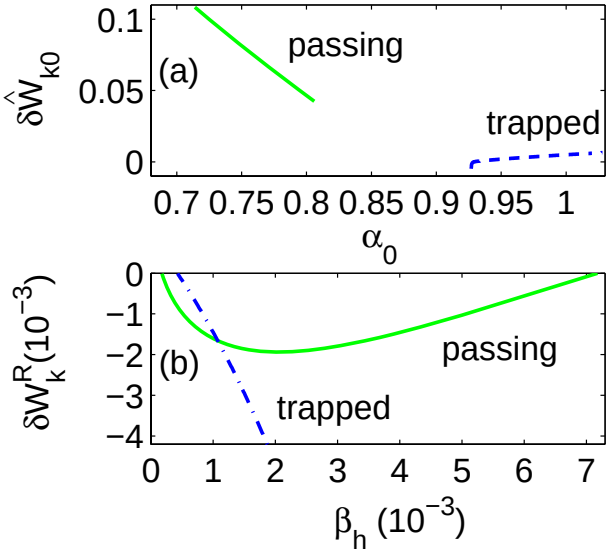

FIG. 6. (a) $\delta\hat{W}_{k0}$ as a function of pitch angle α_0 for trapped (the broken lines) and passing ions (the solid lines) with β_h =0.002 and (b) δW_k^R as a function of β_h with α_0 =0.76 for barely passing ions and α_0 =0.93 for barely trapped ions. The other parameters are σ =2.5, $\hat{r}_0$ =0.72.

5. Conclusions

the internal kink (fishbone) mode induced by barely passing energetic ions is investigated numerically. It is found that the mode is resonantly excited by the energetic ions and the mode frequency is comparable to the toroidal precession frequency ω_d. Therefore the mode frequency is low in the case of positive density gradient $\partial F/\partial r > 0$ dominating case (off-axis NBI deposition) whereas is high in the case of negative density gradient $\partial F/\partial r < 0$ dominating (near-axis NBI deposition), corresponding to the fact that the toroidal precession frequency is inversely proportion to radial position *r*. The most interesting result found in this

work is that there exists a second stable regime for the mode in the higher β_h parameter range and there are two threshold beta values, β_{th1} and β_{th2}. The mode may be excited by barely passing energetic ions in the range of $\beta_{th1} < \beta_h < \beta_{th2}$ only. The results are also confirmed with Nyquist technique. The positive free energy (i.e. the damping term in the dispersion relation) increases with increasing beta of EIs and drives the plasma into the second stabile regime near the second stability threshold beta value. The physics mechanism for the existence of the second stability range is the competition between the driving and damping forces related to magnetic gradient and curvature drifts as well as density gradient. Besides, there exist a minimum density gradient parameter and a minimum deposition position of NBI for the mode to be unstable.

The results of this work may provide a way to reduce or even prevent the loss of NBI energetic ions through fishbone modes and to increase the NBI heating efficiency by adjusting the pitch angle and driving the system into the second stable regime fast enough.

Acknowledgments

The discussions with Drs. J. Q Li, Y. Kishimoto, R. White and L. Chen are gratefully acknowledged. This work is supported by National Basic Research Program of China under grant No. 2008CB717806 , ITER Project in China under grant No. 2009GB105005 and National Magnetic Confinement Fusion Science Program under grant No. 2009GB101002, and also partly supported by the JSPS-CAS Core-University Program in the field of Plasma and Nuclear Fusion.

References

[1] K. McGuire, et al., Phys. Rev. Lett. **50**, 891 (1983).
[2] K. L. Wong, et al., Phys. Rev. Lett. **85**, 996 (2000).
[3] X.T. Ding, et al., Nucl. Fusion. **42**, 491 (2002).
[4] L. Chen and M. N. Rosenbluth, Phys. Rev. Lett. **52**, 1122 (1984).
[5] R. B. White, L. Chen, F. Romanelli, and R. Hay, Phys. Fluids. **28**, 278 (1985).
[6] C. Z. Cheng, Phys. Fluids B. **2**, 1427 (1990).
[7] F. Zonca, et al., Nucl. Fusion. **47**, 1588 (2007).
[8] W. W. Heidbrink, et al., Phys. Rev. Lett. **57**, 835 (1986).
[9] R. B. White, et al., Phys. Rev. Lett. **60**, 2038 (1988).
[10] R. B. White, M. N. Bussac and F. Romanelli, Phys. Rev. Lett. **62**, 539 (1989).
[11] M. N. Rosenbluth, et al., Phys. Rev. Lett. **51**, 1967 (1983).
[12] M. Rosenbluth and M. L. Sloan, Phys. Fluids. **14**, 1725 (1971).
[13] J.W. Connor, R.J. Hastie, and T. J. Martin, Nucl. Fusion. **23**, 1702 (1983).
[14] M. N. Bussac, R. Pellat, D. Edery and J. L. Soule, Phys. Rev. Lett. **34**, 1638 (1975).
[15] Y. Liu, et al., Nucl. Fusion, **45**, S239 (2005).